Talanta 99 (2012) 951–958

Contents lists available at SciVerse ScienceDirect

Talanta

journal homepage: www.elsevier.com/locate/talanta

Development of a novel europium(III) complex-based luminescence probe for time-resolved luminescence imaging of the nitric oxide production in neuron cells

Mingjing Liu, Zhiqiang Ye*, Guilan Wang, Jingli Yuan*

State Key Laboratory of Fine Chemicals, School of Chemistry, Dalian University of Technology, Dalian 116024, PR China

ARTICLE INFO

Article history:
Received 7 June 2012
Received in revised form
20 July 2012
Accepted 25 July 2012
Available online 1 August 2012

Keywords:
Europium complex
Luminescence probe
Cell imaging
Nitric oxide
Time-resolved luminescence

ABSTRACT

Nitric oxide (NO) is a signaling molecule, and plays an important role in some human neuroses. In this work, a novel europium(III) complex, [4′-(3-methylamino-4-aminophenoxy)-2,2′:6′,2″-terpyridine-6,6″-diyl] bis(methylenenitrilo) tetrakis(acetate)-Eu^{3+} (MATTA-Eu^{3+}), has been designed and synthesized as a luminescent probe for the time-resolved luminescence detection of NO. The complex itself is weakly luminescent, but can specifically react with NO under the aerobic conditions to form its triazole derivative, [4′-(3-methyl-4-benzotriazol-6-yl-oxy)-2,2′:6′,2″-terpyridine-6,6″-diyl] bis(methylenenitrilo) tetrakis(acetate)-Eu^{3+} (MBTTA-Eu^{3+}), accompanied by a remarkable luminescence enhancement with a long luminescence lifetime. The luminescence response of the complex to NO is rapid, highly selective and sensitive, and pH-insensitive in aqueous solutions. These properties enable MATTA-Eu^{3+} to be used as a turn-on luminescent probe for the selective recognition and sensitive time-resolved luminescence detection of NO in a wider pH range. The probe-loaded PC12 cells were prepared, and used for the time-resolved luminescence imaging detection of the glutamate-induced NO production in the cells. The result demonstrated the practical utility of the probe for imaging the NO production in neuron cells.

1. Introduction

As an important signaling molecule, nitric oxide (NO) regulates a wide range of physiological and pathophysiological processes in many biological systems. In nervous system, the glutamate-induced neurotoxicity is one of the important mechanisms of ischemic or hypoxic neuronal injury [1]. The activation of *N*-methyl-D-aspartate (NMDA) subtype of glutamate receptors can trigger the entry of Ca^{2+} ions into cells, which binds to calcium–calmodulin (Ca–CaM) to stimulate the activity of NO synthetase (NOS). Because the activated NOS-induced NO production plays an important role in some human neuroses, such as Alzheimer's and Parkinson's diseases [2,3], to monitor the NO production in neuron cells is of great importance for investigating the pathophysiology and generant mechanism of NO in these diseases.

Among various detection methods for NO [4–13], fluorescent probe technique, combining the use of a fluorescence microscopy, is a powerful tool for sensing and imaging the intracellular NO production because of its high sensitivity, selectivity and experimental feasibility. In general, the fluorescent probes for NO are developed by coupling an electron-rich *o*-diaminophenyl group to various fluorophores, since which can both effectively quench the fluorescence of fluorophores by a photoinduced electron transfer (PET) mechanism and specifically react with NO under the aerobic conditions to form the corresponding benzotriazole derivatives, to switch-on the fluorescence of fluorophores [14–18]. Another approach for developing NO fluorescent probe is to link a fluorescence quencher of Cu(II) complex to a fluorophore. After reacting with NO, Cu(II) is reduced to Cu(I) to cause the decomposition of the copper complex, and thus the fluorophore's fluorescence can be restored [19–21].

Though a number of organic-dye-based fluorescent probes for NO have been developed, the fluorescence measurement using these probes suffered from the effects of the autofluorescence from biosamples, scattering lights from the optical components, and the photobleaching of organic fluorophores. In a recent communication we found that a Eu^{3+} complex, {4′-[4-(3,4-diaminophenoxy)phenyl]-2,2′:6′,2″-terpyridine-6,6″-diyl} bis(methylenenitrilo) tetrakis (acetate)-Eu^{3+} (DATTA-Eu^{3+}), could be used as a highly selective probe for the time-resolved luminescence detection of NO in living plant cells and tissues [22]. This probe shows the unique luminescence properties of a Eu^{3+} complex with large Stokes shift, long luminescence lifetime and sharp emission profile, which enable it to be favorably useful for the time-resolved luminescence detection of

* Corresponding authors. Tel./fax: +86 411 84986041.
E-mail addresses: zhiqiangye2001@yahoo.com.cn (Z. Ye), jingliyuan@yahoo.com.cn (J. Yuan).

0039-9140/$ - see front matter © 2012 Elsevier B.V. All rights reserved.
http://dx.doi.org/10.1016/j.talanta.2012.07.064

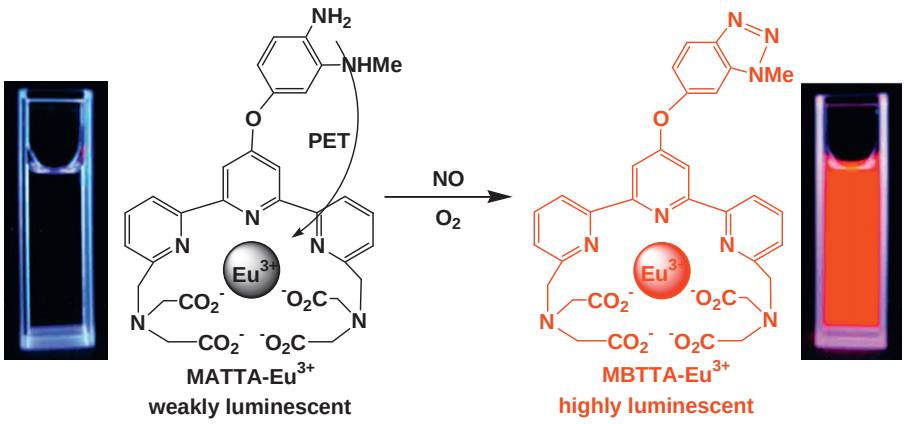

Scheme 1. Luminescence response reaction of MATTA-Eu^{3+} to NO under the aerobic conditions (the photographs show the luminescence colors of the complex aqueous solutions under a 365 nm UV lamp).

NO in complicated biological specimens, since the short-lived autofluorescence and scattering lights can be easily eliminated by the time-resolved detection mode [23,24]. The main disadvantage of the probe is its pH-sensitive luminescence behavior, which limits the probe's availability in a narrow pH range.

To overcome the disadvantage of the NO probe DATTA-Eu^{3+}, in this work, an improved Eu^{3+} complex-based luminescence probe for NO, [4′-(3-methylamino-4-aminophenoxy)-2,2′:6′,2″-terpyridine-6,6″-diyl] bis(methylenenitrilo) tetrakis(acetate)-Eu^{3+} (MATTA-Eu^{3+}), was designed and synthesized for the time-resolved luminescence detection of NO. Because an *o*-amino-methylamino-phenyl group was used instead of *o*-diaminophenyl group for reacting with NO to minimize the protonation of its triazole derivative [15,17] (Scheme 1), the new probe showed a wider pH available range for recognizing and detecting NO. Moreover, the probe displayed rapid luminescence response to NO with high selectivity and sensitivity in aqueous solutions. To image the NO production in neuron cells, the MATTA-Eu^{3+}-loaded PC12 cells were prepared using a previous method [23] by co-incubating the cells with the acetoxymethyl ester of MATTA-Eu^{3+} (AM-MATTA-Eu^{3+}), and then the glutamate-induced NO production in the cells was successfully imaged with time-resolved luminescence mode.

2. Experimental

2.1. Materials and methods

Diethyl 4′-hydroxy-2,2′:6′,2″-terpyridine-6,6″-dicarboxylate (compound **1**) was synthesized according to the literature method [25]. PC12 cells were obtained from Dalian Medical University. Deionized and distilled water was used throughout all the experiments. The stock solutions of NO, $ONOO^-$ and H_2O_2 were prepared and assayed using the previous method [26,27]. Hydroxyl radical ($\cdot OH$) was generated in the Fenton system from ferrous ammonium sulfate and hydrogen peroxide [28]. Singlet oxygen ($^1O_2$) was generated by the reaction of hypochlorite with hydrogen peroxide [29]. Superoxide anion radical (O_2^-) was generated from the xanthine–xanthine oxidase system [30]. The freshly prepared aqueous solutions of NaOCl, $NaNO_2$ and $NaNO_3$ were used as hypochlorite anion (ClO^-), nitrite (NO_2^-) and nitrate (NO_3^-) sources, respectively. Unless otherwise stated, all chemical materials were purchased from commercial sources and used without further purification.

^1H and ^{13}C NMR spectra were recorded on a Bruker Avance spectrometer (400 MHz for ^1H and 100 MHz for ^{13}C). Mass spectra were measured on a HP1100LC/MSD electrospray ionization mass spectrometer (ESI-MS). Elemental analysis was carried out on a Vario-EL CHN analyzer. Absorption spectra were measured on a Perkin-Elmer Lambda 35 UV–vis spectrometer. Time-resolved luminescence spectra were measured on a Perkin-Elmer LS 50B luminescence spectrometer with the conditions of delay time, 0.2 ms; gate time, 0.4 ms; cycle time, 20 ms; excitation slit, 10 nm; and emission slit, 5 nm. The calibration curve (the inset in Fig. 3) for the time-resolved luminescence measurement of NO was measured on a Perkin-Elmer Victor 1420 Multilabel Counter with the conditions of excitation wavelength, 340 nm; emission wavelength, 615 nm; delay time, 0.2 ms; window time (counting time), 0.4 ms; and cycling time, 1.0 ms. The luminescence quantum yields were measured with a previous method [23,28]. The time-resolved luminescence imaging measurements were carried out on a laboratory-use luminescence microscope [31]. The microscope, equipped with a 30 W xenon flash-lamp (Pulse300, Photonic Research Systems Ltd.), UV-2A filters (Nikon, excitation filter, 330–380 nm; dichroic mirror, 400 nm; emission filter, >420 nm) and a time-resolved digital black-and-white CCD camera system (Photonic Research Systems Ltd.), was used for the time-resolved luminescence imaging measurement with the conditions of delay time, 100 μs; gate time, 1000 μs; lamp pulse width, 6 μs; and exposure time, 180 s. The time-resolved luminescence images are shown in pseudo-color treated by a SimplePCI software [31].

2.2. Syntheses of the new Eu^{3+} ligands

Scheme 2 shows the reaction pathways for the synthesis of the new ligands MATTA, MBTTA and AM-MATTA. The experimental details are described as follows.

2.2.1. Synthesis of 2-methylamino-4-fluoronitrobenzene (1)

$MeNH_2$ (30% aqueous solution, 1.0 mL) was carefully added to a suspension of 2,4-difluoronitrobenzene (300 mg, 1.89 mmol) in ethanol (5.0 mL). The solution was stirred for 15 h at 0 °C, and then filtered. After evaporation, the crude product was purified by silica gel chromatography eluted with CH_2Cl_2-hexane (1:6, v/v) to yield the target compound (190 mg, 59%). ^1H NMR ($CDCl_3$, 400 MHz): δ 8.24–8.20 (*m*, 1H), 8.15 (*s*, 1H), 6.49–6.46 (*m*, 1H), 6.40–6.35 (*m*, 1H), 3.01 (*d*, J=4.0 Hz, 3H). ESI-MS (*m*/*z*): 171.1, $[M+H]^+$.

2.2.2. Synthesis of diethyl 4′-(3-methylamino-4-nitrophenoxy)-2,2′:6′,2″-terpyridine-6,6″- dicarboxylate (2)

To a solution of compound **1** (300 mg, 0.76 mmol) in anhydrous *N*,*N*-dimethylformamide (DMF, 5 mL) was added NaH (27 mg, 0.78 mmol) under an argon atmosphere, and the solution was stirred

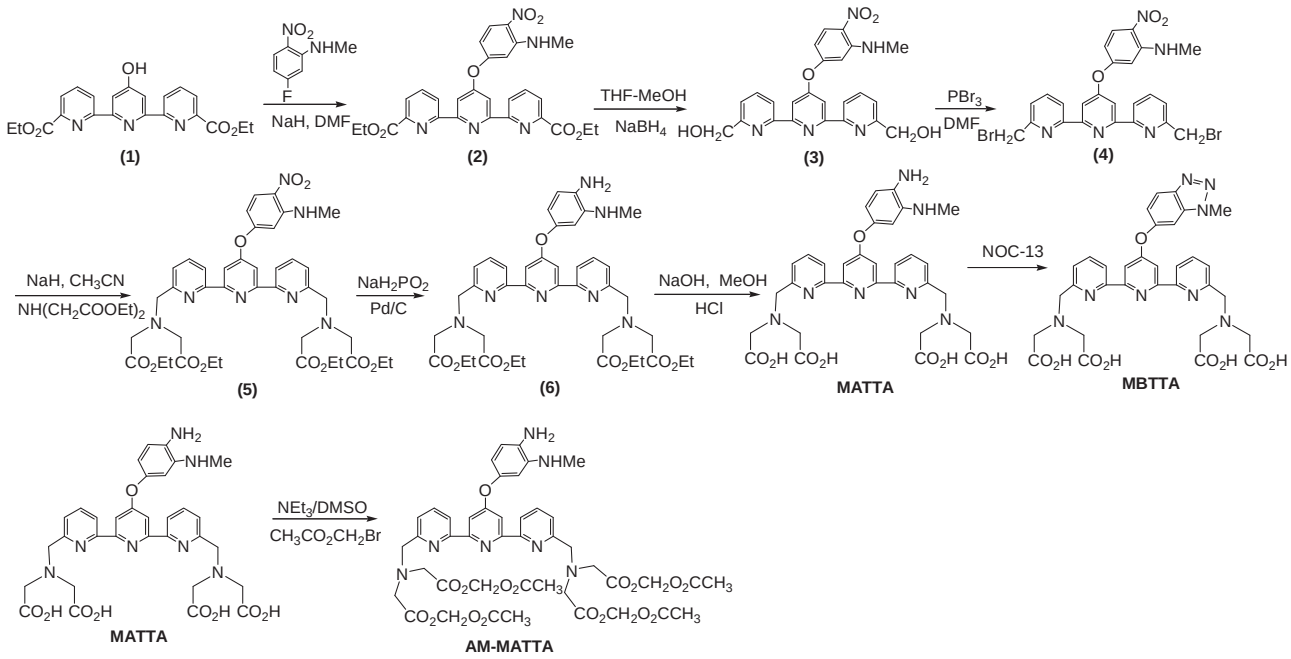

Scheme 2. Reaction pathways for the synthesis of the new ligands MATTA, MBTTA and AM-MATTA. The compound **1** was synthesized according to the literature method [25].

for 60 min at room temperature. After 2-methylamino-4-fluoronitrobenzene (190 mg, 1.11 mmol) and K_2CO_3 (1.0 g, 7.25 mmol) were added, the mixture was stirred at 90 °C for 24 h. The solution was added dropwise into 80 mL of cooled water, and then the mixture was stirred for 30 min. The precipitate of crude product was collected by filtration, and further purified by silica gel chromatography eluted with CH_2Cl_2-MeOH (100:3, v/v) to afford compound **2** (150 mg, 36%). ^{1}H NMR($CDCl_3$, 400 MHz): 8.80 (*d*, *J*=8.0 Hz, 2H), 8.31 (*s*, 2H), 8.28 (*d*, *J*=9.6 Hz, 1H), 8.17 (*d*, *J*=7.6 Hz, 2H), 8.02 (*t*, *J*=8.0 Hz, 2H), 6.59 (*d*, *J*=2.4 Hz, 1H), 6.46–6.43 (*m*, 1H), 4.50–4.44 (*m*, 4H), 3.0 (*d*, *J*=4.0 Hz, 3H), 1.41 (*t*, *J*=8.0 Hz, 6H). ESI-MS (*m*/*z*): 544.2, $[M+H]^+$.

2.2.3. Synthesis of 4′-(3-methylamino-4-nitrophenoxy)-2,2′:6′,2″-terpyridine-6,6″-dimethanol (3)

To a suspension of compound **2** (150 mg, 0.27 mmol) in tetrahydrofuran (THF, 20 mL) was added $NaBH_4$ (64 mg, 1.68 mmol), and then the mixture was refluxed for 1 h. After 2 mL of methanol was added, the solution was refluxed for 1 h and further stirred at room temperature for 5 h. After evaporation, 10 mL of saturated $NaHCO_3$ solution was added, and the mixture was heated to boiling for 10 min. The suspension was poured into 30 mL of ice-water, and the precipitate was filtered and washed with water. After drying, compound **3** was obtained (117 mg, 95%). ^{1}H NMR ($CDCl_3$, 400 MHz): δ 8.58 (*d*, *J*=7.6 Hz, 2H), 8.27 (*d*, *J*=9.2 Hz, 1H), 8.19 (*s*, 2H), 7.96 (*t*, *J*=7.6 Hz, 2H), 7.38 (*d*, *J*=7.6 Hz, 2H), 6.57 (*d*, *J*=2.4 Hz, 1H), 6.41–6.39 (*m*, 1H), 4.88 (*s*, 4H), 3.00 (*d*, *J*=4.0 Hz, 3H). ESI-MS (*m*/*z*): 460.1, $[M+H]^+$.

2.2.4. Synthesis of 6,6″-bis(bromomethyl)-4′-(3-methylamino-4-nitrophenoxy)-2,2′:6′,2″- terpyridine (4)

After a mixture of dry DMF (10 mL) and PBr_3 (300 mg, 1.1 mmol) was stirred at room temperature for 15 min, compound **3** (150 mg, 0.32 mmol) was added, and the mixture was stirred for 24 h at 0 °C. The solution was neutralized with saturated $NaHCO_3$ solution, and the precipitate was filtered and washed with water. The crude product was purified by silica gel chromatography eluted with CH_2Cl_2-MeOH (100:1, v/v) to afford compound **4** (75 mg, 40%). ^{1}H NMR ($CDCl_3$, 400 MHz): δ 8.54 (*d*, *J*=8.0 Hz, 2H), 8.27 (*d*, *J*=9.2 Hz, 1H), 8.21 (*s*, 2H), 7.90 (*t*, *J*=7.6 Hz, 2H), 7.53 (*d*, *J*=8.0 Hz, 2H), 6.59 (*d*, *J*=2.4 Hz, 1H), 6.43–6.41 (*m*, 1H), 5.30 (*s*, 4H), 3.00 (*d*, *J*=4.0 Hz, 3H). ESI-MS (*m*/*z*): 586.0, $[M+H]^+$.

2.2.5. Synthesis of tetraethyl [4′-(3-methylamino-4-nitrophenoxy)-2,2′:6′,2″-terpyridine-6,6″-diyl] bis(methylenenitrilo) tetrakis(acetate) (5)

To a solution of diethyl iminodiacetate (355 mg, 1.88 mmol) in dry acetonitrile (15 mL) and THF (15 mL) was added NaH (58 mg, 1.71 mmol) under an argon atmosphere, and the mixture was stirred for 60 min at room temperature. After compound **4** (500 mg, 0.854 mmol) was added, the mixture was stirred overnight at room temperature, and then filtered. The filtrate was evaporated, and the residue was dissolved in $CHCl_3$ (20 mL). The $CHCl_3$ solution was washed with water (2 × 20 mL), and dried with Na_2SO_4. After evaporation, the crude product was purified by silica gel chromatography eluted with petroleum ether–ethyl acetate (2:1, v/v), and further recrystallized from n-hexane to afford compound **5** (300 mg, 44% yield). ^{1}H NMR ($CDCl_3$, 400 MHz): δ 8.52 (*d*, *J*=7.6 Hz, 2H), 8.25 (*d*, *J*=9.2 Hz, 1H), 8.17 (*s*, 2H), 7.88 (*t*, *J*=7.6 Hz, 2H), 7.69 (*d*, *J*=7.6 Hz, 2H), 6.54 (*d*, *J*=2.4 Hz,1H), 6.41–6.39 (*m*,1H), 4.19–4.13 (*m*, 12H), 3.69 (*s*, 8H), 2.99 (*d*, *J*=4.0 Hz, 3H), 1.26–1.23 (*m*, 12H). ESI-MS (*m*/*z*): 802.3, $[M+H]^+$.

2.2.6. Synthesis of tetraethyl [4′-(3-methylamino-4-aminophenoxy)-2,2′:6′,2″-terpyridine-6,6″- diyl] bis(methylenenitrilo) tetrakis(acetate) (6)

To a mixture of compound **5** (300 mg, 0.37 mmol) and 10% Pd/C (35 mg) in ethanol (30 mL) was added dropwise a solution of NaH_2PO_2 (520 mg, 5.9 mmol) in water (7 mL) under an argon atmosphere. After the mixture was refluxed for 2 h, the Pd/C catalyst was removed by filtration, and then the solvent was evaporated. The residue was dissolved in $CHCl_3$ (20 mL), and the $CHCl_3$ solution was washed with water (2 × 20 mL) and dried with Na_2SO_4. After evaporation, the crude product was purified by silica gel chromatography eluted with petroleum ether–ethyl acetate (1:5, v/v) to afford compound **6** (140 mg, 49% yield).

^{1}H NMR ($CDCl_3$, 400 MHz): δ 8.46 (*d*, *J*=8.0 Hz, 2H), 8.02 (*s*, 2H), 7.82 (*t*, *J*=7.6 Hz, 2H), 7.58 (*d*, *J*=4.0 Hz, 2H), 6.76 (*d*, *J*=8.0 Hz, 1H), 6.50–6.48 (*m*, 2H), 4.17–4.08 (*m*, 12H), 3.65 (*s*, 8H), 2.81 (*s*, 3H), 1.30–1.24 (*m*, 12H). ESI-MS (*m*/*z*): 772.5, $[M+H]^+$.

2.2.7. Synthesis of MATTA

A mixture of compound **6** (140 mg, 0.18 mmol), ethanol (10 mL) and NaOH (150 mg, 3.75 mmol) was stirred at room temperature for 24 h under an argon atmosphere. After evaporation, the residue was dissolved in water (15 mL). To the solution was added dropwise 1 M HCl to adjust the pH to ~3, and then the suspension was stirred for 3 h at room temperature. The precipitate was filtered and washed with water. After drying, the solid was refluxed in dry acetonitrile (20 mL) for 10 min. The product was collected by filtration, and then dried to afford MATTA (40 mg, 33% yield). ^{1}H NMR (DMSO-d_6, 400 MHz): δ 8.47 (*d*, *J*=7.6 Hz, 2H),7.98 (*t*, *J*=7.2 Hz, 2H), 7.90 (*s*, 2H), 7.63 (*d*, *J*=7.2 Hz, 2H), 6.64 (*d*, *J*=8.0 Hz, 1H), 6.33–6.27 (*m*, 2H), 4.03 (*s*, 4H), 3.52 (*s*, 8H), 2.70 (*s*, 3H). ^{13}C NMR (DMSO-d_6, 100 MHz): δ=30.59, 57.79, 59.72, 102.38, 108.25, 108.35, 111.41, 119.71, 123.19, 133.10, 138.25, 139.45, 146.10, 154.63, 157.34, 159.47, 168.09, 174.21, 174.30. Elemental analysis calcd. (%) for $C_{32}H_{33}N_7O_9 \cdot 4.5H_2O$ (MATTA·4.5H_2O): C 51.65, H 5.74, N 13.09; found (%): C 51.89, H 5.67, N 13.24. ESI-MS (*m*/*z*): 660.3, $[M+H]^+$.

2.2.8. Synthesis of MBTTA

To a solution of MATTA (11.1 mg, 15.0 μmol) in 2.0 mL of 0.05 M borate buffers pH 7.4 was added 1-hydroxy-2-oxo-3-(3-amino-propyl)-3-methyl-1-triazene (NOC-13, a NO donor with a half-life of 13.7 min [32], 20.0 mg, 122 μmol). After stirring overnight at room temperature, the solution was used as a stock solution of MBTTA. ESI-MS (*m*/*z*): 669.2 $[M-H]^-$.

2.2.9. Synthesis of the acetoxymethyl ester of MATTA (AM-MATTA)

To a solution of MATTA (11.1 mg, 15.0 μmol) and bromomethyl acetate (61 μL, 618 μmol) in dry DMSO (150 μL) was added dry triethylamine (89 μL, 617 μmol) under an argon atmosphere. After stirring overnight at room temperature, the precipitate was removed by centrifugation. The supernatant was carefully collected and used as the stock solution of AM-MATTA without further purification. ESI-MS (*m*/*z*): 948.7, $[M+H]^+$.

2.3. Reactions of MATTA-Eu^{3+} with different reactive oxygen/nitrogen species

The stock solution of MATTA-Eu^{3+} was prepared by mixing equivalent molar of MATTA and $EuCl_3$ in 0.05 M borate buffer of pH 7.4 at room temperature with stirring. ESI-MS (*m*/*z*): 812.8 $[M+H]^+$, 835.0 $[M+Na]^+$. After the MATTA-Eu^{3+} solution (2.0 μM) was reacted with different reactive oxygen/nitrogen species (30.0 μM) for 30 min in 0.05 M borate buffer of pH 7.4 at room temperature, respectively, the time-resolved emission spectra of the solutions were measured on the Perkin-Elmer LS 50B luminescence spectrometer.

2.4. Luminescence imaging of the glutamate-induced NO production in PC12 cells

PC12 cells were cultured in 1640 medium, supplemented with 10% fetal bovine serum (Corning Incorporated), 1% penicillin and 1% streptomycin (Gibco) at 37 °C in a 5% CO_2—95% air incubator. The cultured cells in a 25 cm^2 glass culture bottle were washed with the culture medium, and then incubated with the culture medium containing 0.5 mM of the freshly prepared AM-MATTA and $EuCl_3$. The bottle was incubated for 2 h at 37 °C in a 5% CO_2—95% air incubator. After washing four times with an isotonic saline solution consisting of 140 mM NaCl, 10 mM glucose and 3.5 mM KCl, the cells were further incubated with the isotonic saline solution containing 2.0 mM glutamate for 4 h, and then subjected to the time-resolved luminescence imaging measurement on the microscope.

3. Results and discussion

3.1. Design, synthesis and luminescence properties of the Eu^{3+} complexes

In a previous work we have demonstrated that a Eu^{3+} complex DATTA-Eu^{3+} can be used as a highly selective and sensitive probe for the time-resolved luminescence detection of NO [22]. To overcome the disadvantage of the pH-sensitive luminescence properties of DATTA-Eu^{3+}, in this work, a new Eu^{3+} complex-based luminescence probe for NO, MATTA-Eu^{3+}, was designed and synthesized. The structure design of the new probe is based on the consideration that the properties of the fluorescence probe using *o*-diaminophenyl as a NO-recognition moiety is strongly affected by pH, while that using *o*-amino-methylamino-phenyl as a NO-recognition moiety is not affected by pH [15,17]. Scheme 2 shows the reaction pathways for the synthesis of MATTA and its reaction product with NO, MBTTA. MATTA was synthesized by a six-step reaction procedure from diethyl 4′-hydroxy-2,2′:6′,2″-terpyridine-6,6″-dicarboxylate, and MBTTA was synthesized by reacting MATTA with NOC-13 in an aqueous buffer. Because the stability of the Eu^{3+} complex moiety of [2,2′:6′,2″-terpyridine-6,6″-diyl] bis(methylenenitrilo) tetrakis(acetate)-Eu^{3+} in neutral aqueous buffers is very high with the

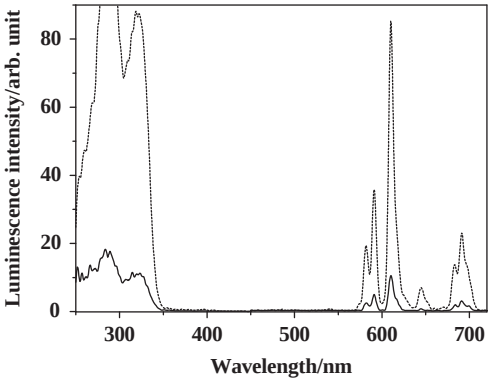

Fig. 1. Time-resolved excitation and emission spectra of MATTA-Eu^{3+} (2.0 μM, solid lines) and MBTTA-Eu^{3+} (2.0 μM, dash lines) in 0.05 M borate buffer of pH 7.4.

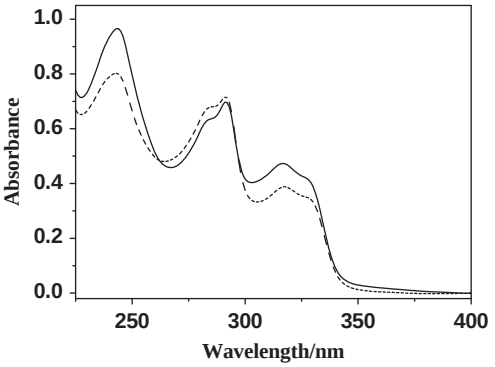

Fig. 2. Absorption spectra of MATTA-Eu^{3+} (20 μM, solid line) and MBTTA-Eu^{3+} (20 μM, dash line) in 0.05 M borate buffer of pH 7.4.

conditional stability constant at 10^{20} level [26,31], the Eu^{3+} complex solutions of MATTA-Eu^{3+} and MBTTA-Eu^{3+} were easily prepared by in-situ mixing equivalent molar of the ligand and Eu^{3+} in 0.05 M borate buffer of pH 7.4. The solutions of two complexes are highly stable at room temperature without changes in their luminescence properties for at least a few weeks. In addition, using the luminescence lifetimes of MATTA-Eu^{3+} and MBTTA-Eu^{3+} in H_2O and D_2O (τ=1.19 ms and 1.20 ms in H_2O and 1.92 ms and 1.89 ms in D_2O for MATTA-Eu^{3+} and MBTTA-Eu^{3+}, respectively), the average number (q) of water molecules in the first coordination sphere of Eu^{3+} ion was calculated from the equation of $q=1.2((1/\tau_{H_2O})-(1/\tau_{D_2O})-0.25)$ [31] to be 0.08 and 0.06, respectively. These results indicate that the new Eu^{3+} complexes have high kinetic and thermodynamic stabilities for the time-resolved luminescence bioassay application.

The luminescence properties of MATTA-Eu^{3+} and MBTTA-Eu^{3+} were determined in 0.05 M borate buffer of pH 7.4. As shown in Fig. 1, although two Eu^{3+} complexes exhibited the same and typical Eu^{3+} excitation and emission patterns with a maximum excitation wavelength at 321 nm, and a main emission peak at 610 nm and several side peaks centered at 583, 593, 646, and 692 nm (corresponding to the $^5D_0 \rightarrow {}^7F_J$ (J=0–4) transitions of Eu^{3+} ion), as expected, the luminescence of MATTA-Eu^{3+} was very weak (ϕ=0.59%), whereas its reaction product with NO, MBTTA-Eu^{3+}, was highly luminescent with ~6.3-fold enhancement in luminescence quantum yield (ϕ=3.77%). This phenomenon can be explained to be attributed to the different PET efficiency in the two Eu^{3+} complexes, higher efficiency in MATTA-Eu^{3+} and lower efficiency in MBTTA-Eu^{3+}. In MATTA-Eu^{3+}, the terpyridine group is an antenna capable of sensitizing the Eu^{3+} luminescence, and the *o*-amino-methylamino-phenyl moiety serves as a switch and its HOMO energy level is higher than the S_0 energy level of the antenna. When the antenna is excited to its singlet state, a PET process from the switch moiety (electron donor) to the antenna (electron acceptor) can occur, which prevents the further energy transfer from the antenna to the central Eu^{3+} ion, resulting in the low luminescence quantum yield of MATTA-Eu^{3+}. After *o*-amino-methylamino-phenyl moiety reacts with NO to form its triazole derivative, the HOMO energy level can be dropped, thus the PET efficiency from the switch moiety to the antenna is remarkably weakened. Thereby, the intramolecular energy transfer from the antenna to the central Eu^{3+} ion is feasible, and the luminescence quantum yield of MBTTA-Eu^{3+} is significantly increased. Indeed, almost the same UV spectrum profiles of MATTA-Eu^{3+} and MBTTA-Eu^{3+} (Fig. 2) supported the above PET mechanism-based explanation.

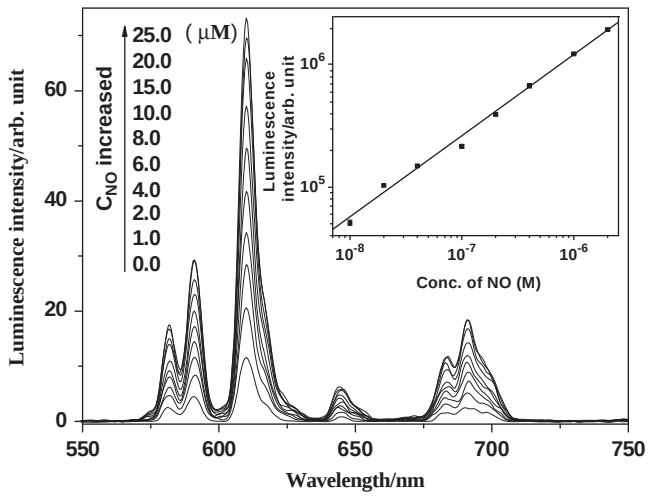

Fig. 3. Time-resolved emission spectra (λ_{ex}=321 nm) of MATTA-Eu^{3+} (2.0 μM) upon reaction with different concentrations of NO at room temperature in 0.05 M borate buffer of pH 7.4. The inset shows the calibration curve measured on a Perkin-Elmer Victor 1420 multilabel counter for the time-resolved luminescence measurement of NO in a low concentration range (0.01–2.0 μM).

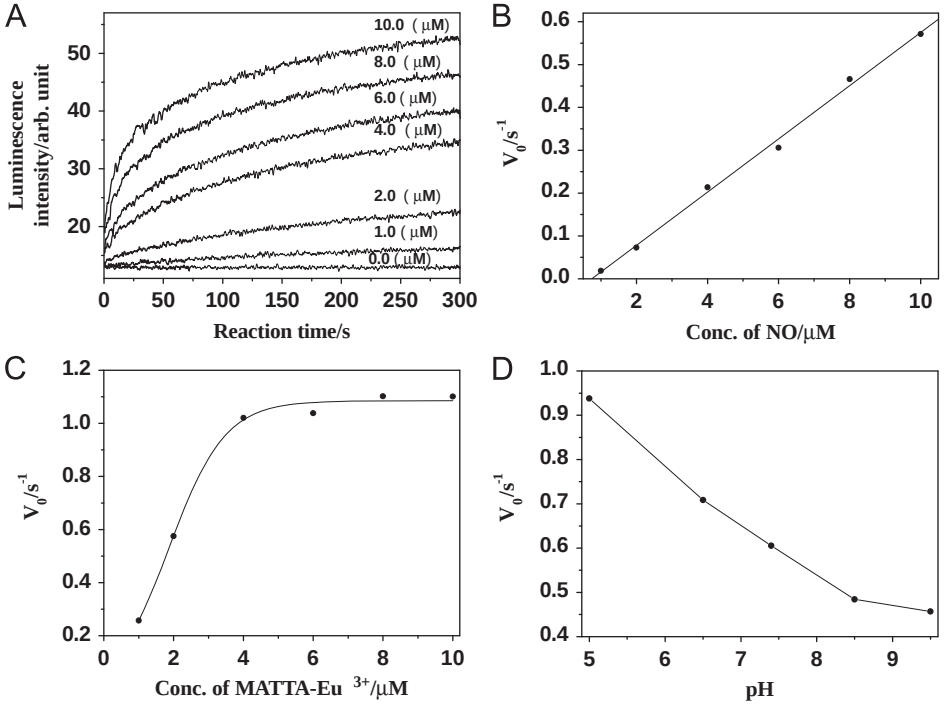

Fig. 4. (A) Temporal dynamics of the luminescence responses of MATTA-Eu^{3+} (2.0 μM) to the additions of different concentrations of NO in 0.05 M borate buffer of pH 7.4. (B) The plot of initial rates (V_0) of the reaction of MATTA-Eu^{3+} (2.0 μM) with NO against the NO concentrations. (C) The plot of initial rates (V_0) of the reaction of MATTA-Eu^{3+} with NO (10.0 μM) against the concentrations of MATTA-Eu^{3+}. (D) The plot of initial rates (V_0) of the reaction of MATTA-Eu^{3+} (2.0 μM) with NO (10.0 μM) in 0.05 M borate buffers with different pHs.

3.2. Luminescence response of MATTA-Eu^{3+} to NO

To quantitatively investigate the luminescence response of MATTA-Eu^{3+} to NO in aqueous media, a luminescence titration experiment of NO using MATTA-Eu^{3+} (2.0 μM) as a probe was carried out in 0.05 M borate buffer of pH 7.4. As shown in Fig. 3, upon additions of different concentrations of NO, the luminescence intensity of the probe showed sensitive dose-dependent enhancement with the increase of NO concentration. The solutions with low NO concentrations (0.01–2.0 μM) in a 96-well microtiter plate were further measured on a more sensitive time-gated luminescence counter, Perkin Elmer Victor 1420 Multilabel Counter. The calibration curve with a good linearity was obtained by plotting log(signal) against log C_{NO} (the inset in Fig. 3). The detection limit for NO, calculated as the concentration corresponding to triple standard deviations of the background signal, is 2.0 nM, which is at the same level compared to those of other highly sensitive NO probes based on a fluorescein derivative (detection limit, 5 nM) [16] and DATTA-Eu^{3+} (detection limit, 8.4 nM) [22], indicating that MATTA-Eu^{3+} can be used as a probe for highly sensitive time-resolved luminescence detection of NO in aqueous media.

The luminescence response dynamics of MATTA-Eu^{3+} to NO was examined by real-time monitoring the time-resolved luminescence intensity change of the probe at 610 nm with excitation at 321 nm. Fig. 4A shows the luminescence response kinetic curves of MATTA-Eu^{3+} (2.0 μM) to the additions of different concentrations of NO in 0.05 M borate buffer of pH 7.4. In the absence of NO, the probe showed only very weak luminescence without the intensity changes.

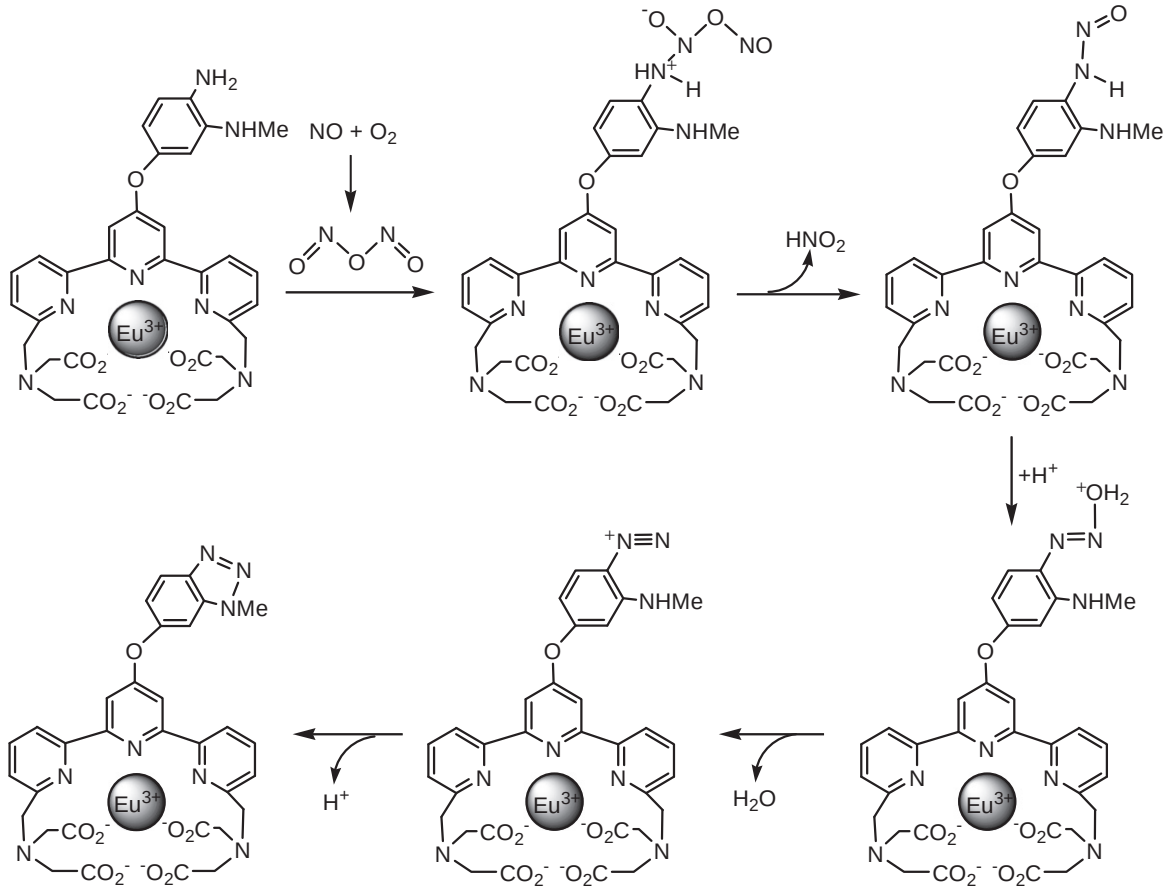

Scheme 3. Reaction mechanism leading to the heterocycle-ring closure reaction between MATTA-Eu^{3+} and NO under the aerobic conditions.

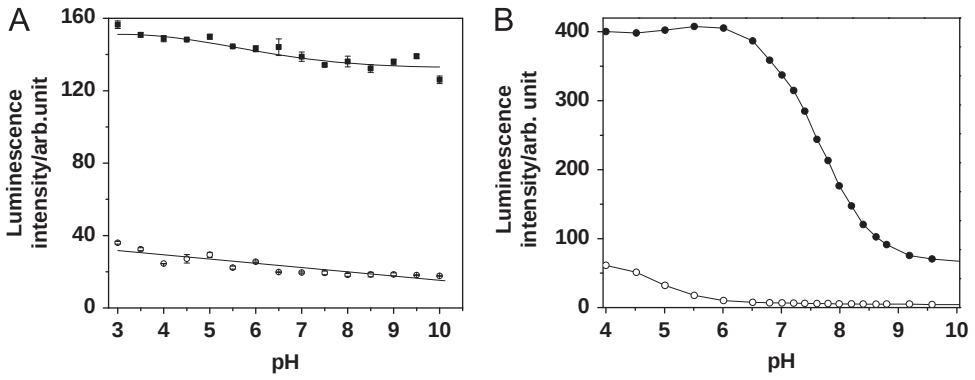

Fig. 5. Effects of pH on the luminescence intensities of MATTA-Eu^{3+} and MBTTA-Eu^{3+} (A, 4.0 μM, ○: MATTA-Eu^{3+}; ●: MBTTA-Eu^{3+}) as well as DATTA-Eu^{3+} and BPTTA-Eu^{3+} (B, 2.0 μM, ○: DATTA-Eu^{3+}; ●: BPTTA-Eu^{3+}) in 0.05 M borate buffers with different pHs.

Upon the addition of NO, the luminescence intensity of the probe was rapidly increased, and reached to the maximum value within ~5 min. To further investigate the effects of experimental conditions on the luminescence response reaction rate of MATTA-Eu^{3+} to NO, the effects of the reactant concentration and pH on the initial rates of the reaction were evaluated. As shown in Fig. 4B–D, the initial rate was significantly increased with the increase of the reactant concentration, whereas the pH increase caused the decrease of the reaction initial rate. Scheme 3 shows the reaction mechanism leading to the heterocycle-ring closure reaction between MATTA-Eu^{3+} and NO under the aerobic conditions [33]. It can be found that lower pH is beneficial to the separations of HNO_2 and H_2O from the complex molecule, and thereby the reaction rate is increased with the pH decrease.

To investigate the effect of pH on the luminescence response of MATTA-Eu^{3+} to NO, the time-resolved luminescence intensities of MATTA-Eu^{3+} and MBTTA-Eu^{3+} in 0.05 M borate buffers with different pHs (4–10) were determined, and the results were compared with those of previously reported Eu^{3+} complex-based NO probe and its NO-reaction product, DATTA-Eu^{3+} and {4′-[4-(benzotriazol-6-yl-oxy)phenyl]-2,2′:6′,2″-terpyridine-6,6″-diyl} bis(methylenenitrilo) tetrakis(acetate)-Eu^{3+} (BPTTA-Eu^{3+}) [22]. As shown in Fig. 5, compared to the strong effects of pH on the luminescence intensities of DATTA-Eu^{3+} and BPTTA-Eu^{3+} (especially in the range of pH 6–9) (Fig. 5B), the effects of pH on the luminescence intensities of MATTA-Eu^{3+} and MBTTA-Eu^{3+} (Fig. 5A) are remarkably weakened. This significant improvement, attributed to the use of *o*-amino-methylamino-phenyl group instead of *o*-diaminophenyl group for recognizing NO, enables the new probe to be used for detecting NO in a wider pH range.

Because some reactive oxygen/nitrogen species, cations and anions often coexist with NO in biosystems [11–13,34,35], the luminescence intensities of the products of MATTA-Eu^{3+} reacted with different reactive oxygen/nitrogen species in 0.05 M borate buffer of pH 7.4 were determined to evaluate the response reaction specificity of MATTA-Eu^{3+} to NO. As shown in Fig. 6A, the luminescence intensity of MATTA-Eu^{3+} did not response noticeably to H_2O_2, NO_3^-, NO_2^-, O_2^-, $ONOO^-$, $^1O_2$, ClO^- and $\cdot OH$, whereas a strong luminescence enhancement was observed after the probe was reacted with NO. In addition, the luminescence intensities of MATTA-Eu^{3+} and MBTTA-Eu^{3+} in the presence of various cations and anions were not remarkably changed (Fig. 6B and C). All of these results indicate that MATTA-Eu^{3+} can be used as a highly specific "turn-on" luminescent probe for the time-resolved luminescence detection of NO.

3.3. Time-resolved luminescence imaging of the glutamate-induced NO production in PC12 cells

In neuron cells, it has been reported that the excessive activation of NO synthase can be induced by glutamate, which produces excessive NO to lead to an increase in the cytosolic Ca^{2+} concentration and cell death [36]. To evaluate the availability of MATTA-Eu^{3+} as a time-resolved luminescence probe for imaging the glutamate-induced NO production in neuron cells, the MATTA-Eu^{3+}-loaded PC12 cells were prepared by co-incubating the cells with the cell-membrane permeable form of MATTA-Eu^{3+}, acetoxymethyl ester of MATTA-Eu^{3+}, according to a previous method [23,26]. After the cells were further incubated in the presence of glutamate, the luminescence imaging measurement was carried out with time-resolved mode.

Fig. 7 shows the time-resolved luminescence images of the MATTA-Eu^{3+}-loaded PC12 cells before and after the glutamate treatment. Compared to the weak luminescence signals from the cells before the glutamate treatment (Fig. 7A), strong luminescence signals from the cells after the glutamate treatment (Fig. 7B) indicated that the NO production was induced by glutamate. To confirm that the luminescence signals from the cells were attributed to the NO production, a control experiment was carried out by

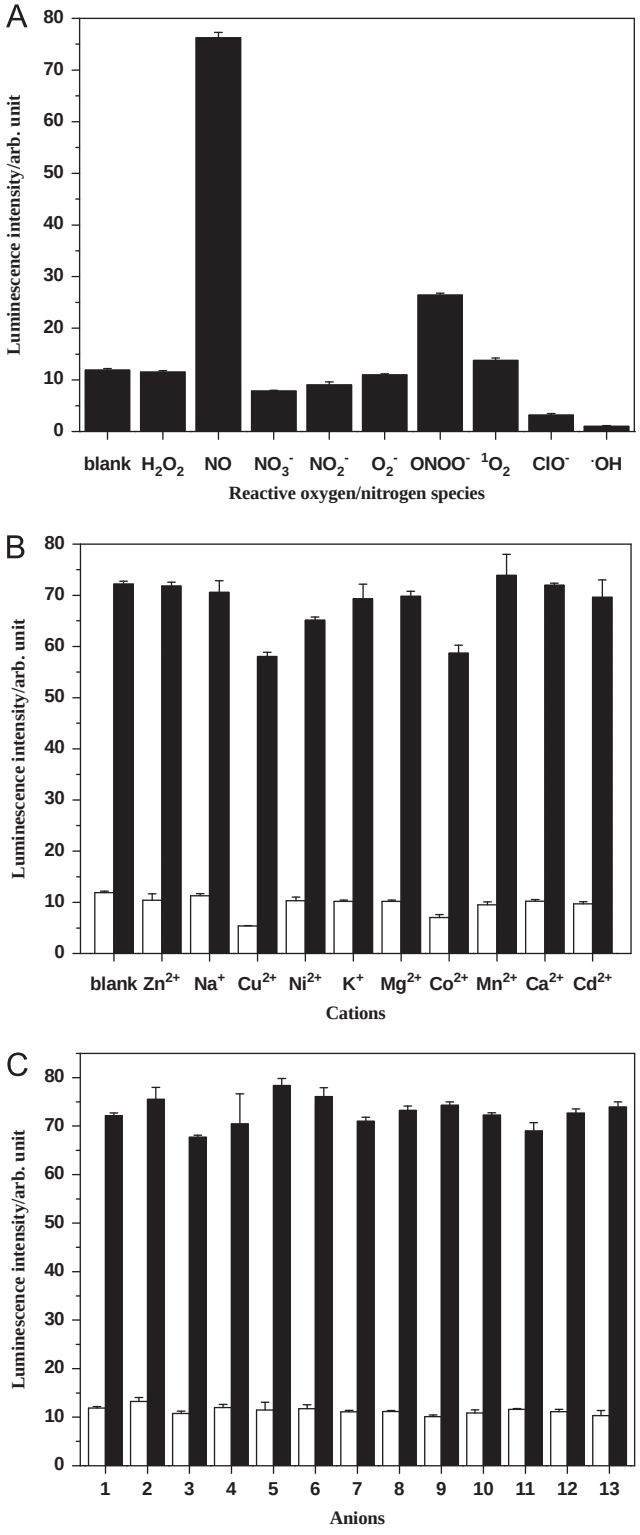

Fig. 6. (A) Luminescence intensities of the products of MATTA-Eu^{3+} (2.0 μM) reacted with different reactive oxygen/nitrogen species (30 μM) in 0.05 M borate buffer of pH 7.4. (B) Luminescence intensities of MATTA-Eu^{3+} (2.0 μM, blank bar) and MBTTA-Eu^{3+} (2.0 μM, black bar) in the presence of different cations (2.0 μM) in 0.05 M borate buffer of pH 7.4. (C) Luminescence intensities of MATTA-Eu^{3+} (2.0 μM, blank bar) and MBTTA-Eu^{3+} (2.0 μM, black bar) in the presence of different anions (30 μM, 1, blank; 2, $P_2O_7^{4-}$; 3, I^-; 4, CO_3^{2-}; 5, AcO^-; 6, Br^-; 7, SO_4^{2-}; 8, Cl^-; 9, F^-; 10, PO_4^{3-}; 11, S^{2-}; 12, oxalate; 13, citrate) in 0.05 M borate buffer of pH 7.4.

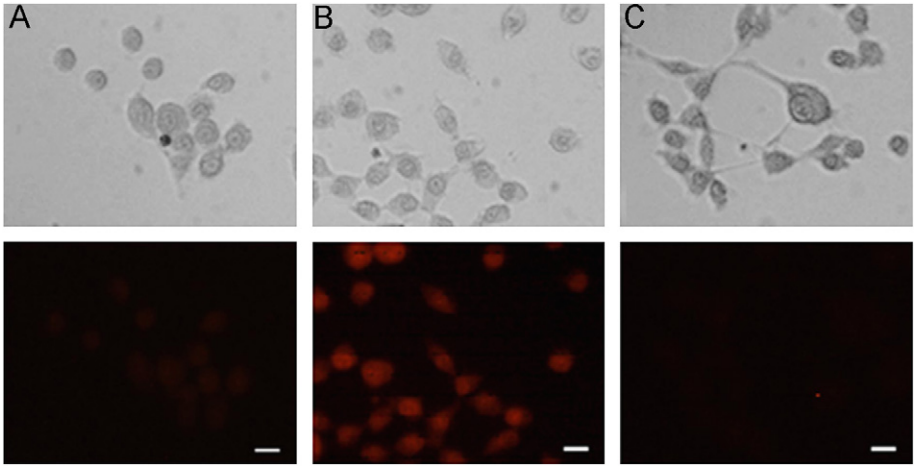

Fig. 7. Bright-field (top) and time-resolved luminescence (bottom, excitation filter: 330–380 nm) images of the MATTA-Eu^{3+}-loaded PC12 cells before and after the glutamate treatment. A: the MATTA-Eu^{3+}-loaded PC12 cells; B: the MATTA-Eu^{3+}-loaded PC12 cells were incubated with glutamate (2.0 mM) for 4 h; C: the MATTA-Eu^{3+}-loaded PC12 cells were incubated with glutamate (2.0 mM) and c-PTIO (0.2 mM) for 4 h. Scale bar: 10 μm.

incubating the MATTA-Eu^{3+}-loaded PC12 cells in the presence of glutamate and a NO scavenger [37], 2-(4-carboxyphenyl)-4,4,5,5-tetramethylimidazoline-1-oxyl-3-oxide (c-PTIO), and then the cells were imaged. In this case, the red luminescence from the cells disappeared (Fig. 7C), which demonstrates that the luminescence signals from the glutamate-treated cells are really attributed to the NO production, and suggests that MATTA-Eu^{3+} could be a useful time-resolved luminescence probe for investigating the biological roles of NO in neuron cells.

4. Conclusions

In this work, by incorporating a *o*-amino-methylamino-phenyl group into a Eu^{3+} complex luminophore (2,2′:6′,2″-terpyridine-6,6″-diyl) bis(methylenenitrilo) tetrakis(acetate)-Eu^{3+}, a unique Eu^{3+} complex-based "turn-on" luminescence probe specific for NO, MATTA-Eu^{3+}, was successfully developed, and used for the time-resolved luminescence imaging detection of the glutamate-induced NO production in PC12 cells. The advantages of good water solubility, high sensitivity and kinetic and thermodynamic stabilities, wide pH available range, and the applicability for time-resolved luminescence measurement enable the probe to be used for detecting NO in complicated biological systems, which would be a useful tool for investigating the pathogenic roles of NO in various biological systems.

Acknowledgment

The present work was supported by the National Natural Science Foundation of China (no. 20835001).

References

[1] D.W. Choi, Neuron 1 (1998) 623.
[2] L. Nowak, P. Bregestovski, P. Ascher, A. Herbet, A. Prochiantz, Nature 307 (1984) 462.
[3] S.E. Craven, D.S. Bredt, Cell 93 (1998) 495.
[4] K. Ichimori, H. Ishida, M. Fukahori, H. Nakazawa, E. Murakami, Rev. Sci. Instrum. 65 (1994) 2714.
[5] Y. Katayama, N. Soh, M. Maeda, ChemPhysChem 2 (2001) 655.
[6] T. Malinski, Z. Taha, Nature 358 (1992) 676.
[7] L.E. McQuade, S.J. Lippard, Curr. Opinion Chem. Biol. 14 (2009) 1.
[8] P. Mordvintcev, A. Mülsch, R. Busse, A. Vanin, Anal. Biochem. 199 (1991) 142.
[9] R.W. Nims, J.F. Darbyshire, J.E. Saavedra, D. Christodoulou, I. Hanbauer, G.W. Cox, M.B. Grisham, F. Laval, J.A. Cook, M.C. Krishna, D.A. Wink, Methods 7 (1995) 48.
[10] L.A. Ridnour, J.E. Sim, M.A. Hayward, D.A. Wink, S.M. Martin, G.R. Buettner, D.R. Spitz, Anal. Biochem. 281 (2000) 223.
[11] D.A. Riccio, M.H. Schoenfisch, Chem. Soc. Rev. 41 (2012) 3731.
[12] A.W. Carpenter, M.H. Schoenfisch, Chem. Soc. Rev. 41 (2012) 3742.
[13] P.N. Coneski, M.H. Schoenfisch, Chem. Soc. Rev. 41 (2012) 3753.
[14] Y. Gabe, Y. Urano, K. Kikuchi, H. Kojima, T. Nagano, J. Am. Chem. Soc. 126 (2004) 3357.
[15] Y. Hirata, T. Nagano, Anal. Chem. 70 (1998) 2446.
[16] H. Kojima, N. Nakatsubo, K. Kikuchi, S. Kawahara, Y. Kirino, H. Nagoshi, H. Kojima, Y. Urano, K. Kikuchi, T. Higuchi, Y. Hirata, T. Nagano, Angew. Chem. Int. Ed. 38 (1999) 3209.
[17] H. Kojima, M. Hirotani, N. Nakatsubo, K. Kikuchi, Y. Urano, T. Higuchi, Y. Hirata, T. Nagano, Anal. Chem. 73 (2001) 1967.
[18] E. Sasaki, H. Kojima, H. Nishimatsu, Y. Urano, K. Kikuchi, Y. Hirata, T. Nagano, J. Am. Chem. Soc. 127 (2005) 3684.
[19] X.Y. Hu, J. Wang, X. Zhu, D.P. Dong, X.L. Zhang, S. Wu, C.Y. Duan, Chem. Commun. 47 (2011) 11507.
[20] M.H. Lim, B.A. Wong, W.H. Pitcock, D. Mokshagundam, M.H. Baik, S.J. Lippard, J. Am. Chem. Soc. 128 (2006) 14364.
[21] M.H. Lim, D. Xu, S.J. Lippard, Nat. Chem. Biol. 2 (2006) 375.
[22] Y.G. Chen, W.H. Guo, Z.Q. Ye, G.L. Wang, J.L. Yuan, Chem. Commun. 47 (2011) 6266.
[23] G.F. Cui, Z.Q. Ye, J.X. Chen, G.L. Wang, J.L. Yuan, Talanta 84 (2011) 971.
[24] M.J. Liu, Z.Q. Ye, G.L. Wang, J.L. Yuan, Talanta 91 (2012) 116.
[25] P. Kadjane, C. Platas-Iglesias, R. Ziessel, L.J. Charbonnière, Dalton Trans. (2009) 5688.
[26] C.H. Song, Z.Q. Ye, G.L. Wang, J.L. Yuan, Y.F. Guan, Chem. Eur. J. 16 (2010) 6464.
[27] R. Zhang, Z.Q. Ye, G.L. Wang, W.Z. Zhang, J.L. Yuan, Chem. Eur. J. 16 (2010) 6884.
[28] K. Setsukinai, Y. Urano, K. Kakinuma, H.J. Majima, T. Nagano, J. Biol. Chem. 278 (2003) 3170.
[29] A.M. Held, D.J. Halko, J.K. Hurst, J. Am. Chem. Soc. 100 (1978) 5732.
[30] K.H. Xu, X. Liu, B. Tang, G.W. Yang, Y. Yang, L.G. An, Chem.-Eur. J. 13 (2007) 1411.
[31] B. Song, G.L. Wang, M.Q. Tan, J.L. Yuan, J. Am. Chem. Soc. 128 (2006) 13442.
[32] J.A. Hrabie, J.R. Klose, D.A. Wink, L.K. Keefer, J. Org. Chem. 58 (1993) 1472.
[33] A. Ghosh, P. Das, S. Saha, T. Banerjee, H.B. Bhatt, A. Das, Inorg. Chim. Acta 732 (2011) 115.
[34] B.C. Dickinson, C.J. Chang, Nat. Chem. Biol. 7 (2011) 504.
[35] A. Gomes, E. Fernandes, J.L.F.C. Lima, J. Biochem. Biophys. Methods 65 (2005) 45.
[36] M. Yamauchi, K. Omote, T. Ninomiya, Brain Res. 780 (1998) 253.
[37] K.S. Gould, O. Lamotte, A. Klinguer, A. Pugin, D. Wendehenne, Plant Cell Environ. 26 (2003) 1851.